A Growing Toolbox to Image Gene Expression in Single Cells: Sensitive Approaches for Demanding Challenges

Xavier Pichon, Mounia Lagha, Florian 'floyd' Mueller, Edouard Bertrand

CellPress

Molecular Cell
Technology Review

A Growing Toolbox to Image Gene Expression in Single Cells: Sensitive Approaches for Demanding Challenges

Xavier Pichon,[1,2] Mounia Lagha,[1] Florian Mueller,[4] and Edouard Bertrand[1,2,3,*]
[1]Institut de Génétique Moléculaire de Montpellier, Université de Montpellier, CNRS, Montpellier, France
[2]Equipe labélisée Ligue Nationale Contre le Cancer, Montpellier, France
[3]Department of Anatomy and Structural Biology, Albert Einstein College of Medicine, Bronx, NY, USA
[4]Unité Imagerie et Modélisation, Institut Pasteur and CNRS UMR 3691, 28 rue du Docteur Roux, 75015 Paris, France
*Correspondence: edouard.bertrand@igmm.cnrs.fr
https://doi.org/10.1016/j.molcel.2018.07.022

The spatiotemporal regulation of gene expression is key to many biological processes. Recent imaging approaches opened exciting perspectives for understanding the intricate mechanisms regulating RNA metabolism, from synthesis to decay. Imaging techniques allow their observation at high spatial and temporal resolution, while keeping cellular morphology and micro-environment intact. Here, we focus on approaches for imaging single RNA molecules in cells, tissues, and embryos. In fixed cells, the rapid development of smFISH multiplexing opens the way to large-scale single-molecule studies, while in live cells, gene expression can be observed in real time in its native context. We highlight the strengths and limitations of these methods, as well as future challenges. We present how they advanced our understanding of gene expression heterogeneity and bursting, as well as the spatiotemporal aspects of splicing, translation, and RNA decay. These insights yield a dynamic and stochastic view of gene expression in single cells.

Introduction

"Seeing is believing and believing is knowing and knowing beats unknowing and the unknown"—Philip Roth. Imaging biological processes has revolutionized our ability to grasp the mechanisms of life. In particular, the development of single-molecule approaches in fixed and live cells opened new avenues to understand gene expression from transcription to RNA decay. *In situ* hybridization (ISH) can determine where specific RNAs locate in a cell or an organism, establish where RNA processing reactions take place, and measure cell-to-cell variation in gene expression. In parallel, many techniques can now image RNA and protein in live cells, giving direct access to the temporal dimension. Imaging approaches have the unique advantage of preserving cell state, morphology, and microenvironment. They revealed the dynamic and stochastic nature of gene expression at the level of single cells, and combined with image analysis and mathematical modeling, they provided unprecedented understanding of gene expression mechanisms. In the first part of this review, we present the technical developments available to image RNA metabolism at the single-molecule level. In the second part, we summarize key recent findings in transcriptional noise and in the spatiotemporal dynamics of splicing, translation, and decay, and outline current developments and challenges.

Imaging Single RNAs in Fixed Cells

Standard smFISH Techniques

ISH was invented in 1969 (Gall and Pardue, 1969) and a major breakthrough was accomplished by the Singer lab in 1998, which reported the detection of single RNA molecules in fixed cells (Femino et al., 1998). In this technique, named single-molecule fluorescent ISH (smFISH), multiple fluorescent oligonucleotides are hybridized to a target RNA, allowing detection of single molecules as diffraction-limited spots under a wide-field microscope (Figure 1). Using many probes yields high signal-to-noise ratios because non-specific signals stem from single oligonucleotides while specific signals result from many probes. Today, most smFISH variants still use multiple oligonucleotides per RNA target, from 10 to 50 (Femino et al., 1998; Raj et al., 2008; Figure 2A). Indirect labeling schemes were also developed in which the primary probes are non-fluorescent but carry a common extra sequence named the *readout* (Figures 2B–2E). This sequence is hybridized to a secondary fluorescent oligonucleotide, providing flexibility in the labels and allowing synthesis of primary probes at low cost (Chen et al., 2015; Choi et al., 2010; Sinnamon and Czaplinski, 2014; Tsanov et al., 2016; Wang et al., 2012; Figure 2B). A good signal is often obtained with 24 oligonucleotides and smFISH is compatible with GFP detection and immuno-staining (Fusco et al., 2003).

Signal Amplification and Contrast Improvements

In optically challenging samples, smFISH may require amplification. Colorimetric and fluorescent enzymatic methods can be used, but DNA-based amplification schemes provide better signals (Sylwestrak et al., 2016). FISH-STICs and branched DNA (bDNA) are related techniques that involve successive hybridizations of pre-amplifiers, amplifiers, and detector oligonucleotides to the readout sequence of unlabeled primary probes (Sinnamon and Czaplinski, 2014; Wang et al., 2012; Figures 2C and 2D). Hybridization chain reaction (HCR) involves the continuous binding of two complementary hairpins on the readout and longer hybridization duration yields more amplification (Choi et al., 2010; Figure 2E). These methods yield 10- to 100-fold signal enhancement but at the cost of more complex experimental workflows.

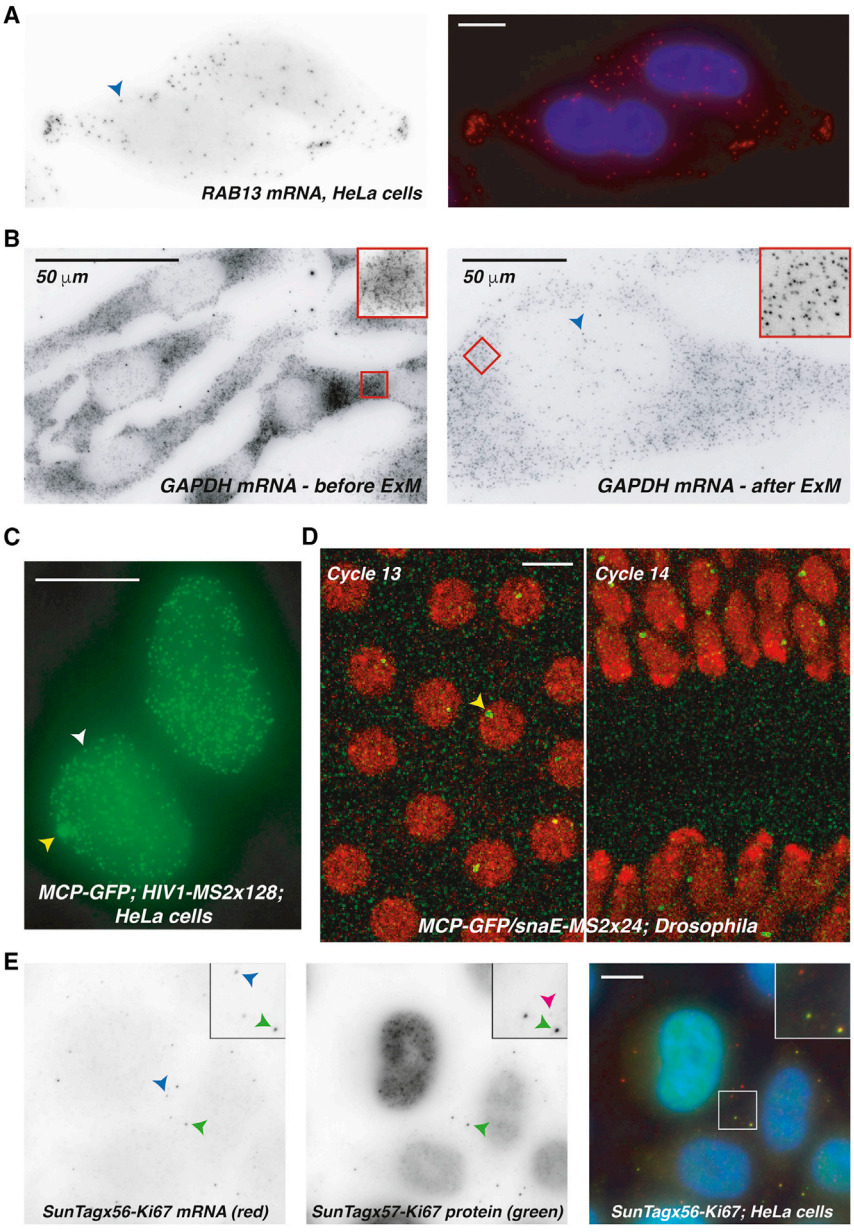

Figure 1. Visualization of RNA and RNA Metabolism in Fixed and Live Cells

(A) Detection of *RAB13* mRNA by smFISH in HeLa cells. Blue arrowhead: a single mRNA molecule. Right panel: DNA is in blue and *RAB13* mRNA in red. *RAB13* mRNAs accumulate at the cell periphery (see Mili et al., 2008). Scale bar, 10 μm.

(B) Expansion microscopy (ExM) coupled to smFISH. *GAPDH* mRNA is detected by smFISH in HeLa cells. Blue arrowhead, a single mRNA. Left, before expansion; right, after expansion. Inset: zoom on the boxed area. Individual mRNAs can be resolved even in dense regions after expansion.

(C) Detection of MS2-tagged pre-mRNA in live HeLa cells. A reporter gene driven by the HIV-1 promoter and carrying 128 MS2 stem-loops in its intron is expressed in a HeLa cell line expressing the MCP-GFP protein. White arrow, a single pre-mRNA; yellow arrow, a transcription site. Scale bar, 10 μm.

(D) Detection of MS2-tagged mRNA in live *Drosophila* embryos. A reporter tagged with 24 MS2 stem-loops under the control of the sna enhancer and promoter is expressed in a strain maternally expressing MCP-GFP (green). Yellow arrow, transcription site; red, nuclei labeled with histone-RFP. Scale bar, 7 μm.

(E) Translation of single mRNPs in fixed cells. HeLa cells expressing an scFv-sfGFP (green and middle panel) and a SunTagx56-Ki67 reporter mRNA (red and left panel). DNA is in blue (right panel). Dark blue arrowheads, untranslated mRNAs; green arrowheads, translated mRNAs; pink arrowhead, a single molecule of SunTag-Ki67 protein. Scale bar, 10 μm.

Amplification is also not uniform across RNAs, potentially confounding RNA aggregates with bright single molecules. Another way of improving contrasts is to use clearing techniques (Long et al., 2017; Moffitt et al., 2016; Shah et al., 2016; Sylwestrak et al., 2016). In general, these different approaches are well suited for imaging with low numerical aperture objectives, as well as in samples that are thick or with high background fluorescence such as embryos or tissues.

Amplification Systems for Short RNAs

RNAs shorter than 0.5–1 kb are difficult to visualize because they cannot bind many probes. Yet many non-coding RNAs and alternative exons are in this length range or shorter. Amplification systems optimized for specificity are well suited for short RNAs. Padlock probes can be covalently closed and amplified only when they bind to the correct target RNA (Larsson et al., 2010; Rouhanifard et al., 2017; Figure 2F). Similarly, the bDNA approach requires the binding of two contiguous pre-amplifiers for successful amplification (Wang et al., 2012; Figure 2D). The limitations of these approaches reside in their long protocols and in the small number of probes that lowers the detection rate; for instance, if probe binding sites are not accessible in all RNA molecules. The high amplification can also create false positives. These methods are, however, powerful and can detect even single microRNA (miRNA) molecules (Larsson et al., 2010).

Large-Scale and Multiplexed smFISH

The first large-scale FISH study was performed in *Drosophila* embryos (Lécuyer et al., 2007). The approach did not reach single-molecule sensitivity but nevertheless led to a remarkable discovery. Indeed, 70% of the 2,300 analyzed mRNAs displayed specific sub-cellular localization patterns, thus revealing that RNA localization is widespread in this organism. In cultured cells, many RNAs are present in few copies per cell and their detection thus requires single-molecule sensitivity. The first systematic smFISH study analyzed 900 human mRNAs with bDNA amplification and low-magnification objectives, while oligonucleotide probes were synthesized individually (Battich et al., 2013).

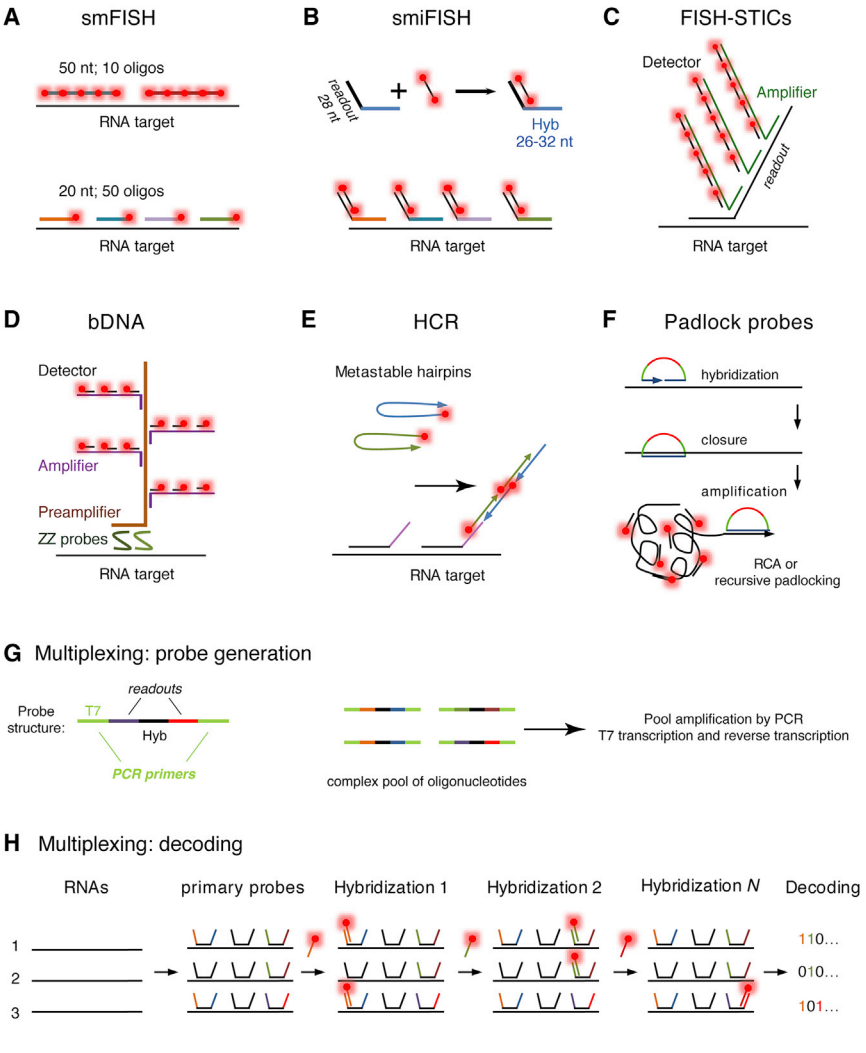

Figure 2. Detection of Single RNAs in Fixed Cells

(A) SmFISH. Top: original smFISH design with 10 oligonucleotides, each 50 bases long and labeled with 5 fluorophores (red). Bottom: more recent design with 50 oligonucleotides, each 20 bases long and labeled with a single fluorophore.

(B) Indirect labeling by smiFISH. A labeled secondary probe is pre-hybridized to 24 primary probes (top). The resulting duplexes are hybridized with cellular RNAs (bottom).

(C) FISH-STICs. Primary probes hybridize to cellular RNAs and are labeled with three amplifier oligonucleotides (green), each of which binds five fluorescent detector oligonucleotides.

(D) Branched DNA (bDNA) smFISH. Comparable to (C), except that the primary probes are pairs of contiguous oligonucleotides and binding of both is required for hybridization with the pre-amplifier.

(E) Hybridization chain reaction (HCR). Two oligonucleotides form metastable hairpins (blue and green) and self-assemble into long polymers in the presence of the readout sequence, which acts as an initiator.

(F) Padlock FISH. A padlock probe (green, blue, and red) takes a circular topology upon binding to target RNAs or cDNAs, and can then be covalently closed. Amplification is achieved by a rolling circle mechanism (RCA), or recursive padlock hybridization (not shown).

(G) Probe generation for multiplexed smFISH. Left: structure of the primary probes. T7: T7 promoter for *in vitro* transcription.

(H) Multiplexed smFISH. Primary probes contain two readout sequences. These are detected by successive rounds of hybridization and they together form a code that allows identification of the bound cellular RNAs.

A cost-effective strategy to scale up smFISH is multiplexing. Current implementations, named merFISH and seqFISH (Chen et al., 2015; Lubeck et al., 2014), allow the detection of up to 10,000 RNA species in the same cell, opening the door to image-based transcriptomics (Shah et al., 2018). These methods can reveal RNA localization and nuclear organization, identify co-regulated genes, and characterize new cell types (Chen et al., 2015; Shah et al., 2016, 2018). Probes are generated by parallel on-chip synthesis, yielding mixtures of 10,000 to 100,000 oligonucleotides. Probes are then amplified by PCR and converted to single strand by *in vitro* transcription and reverse transcription (Figure 2G). High levels of multiplexing require encoding schemes, in which the probes for a single RNA species carry multiple readout sequences (Figure 2H). These are detected by sequential rounds of hybridization, using either one or multiple colors at a time (Chen et al., 2015; Lubeck et al., 2014; Shah et al., 2018). Each readout sequence is analogous to a digital bit, and in theory, n readouts allow for $2^n - 1$ codes (i.e., RNA species; Figure 2H). The encoding capacity is, however, voluntarily reduced to include error correction schemes, such that the correct code can still be identified with single reading errors. Another limitation is that encoding requires all transcripts to be spatially separated, a condition no longer met if abundant or numerous transcripts are imaged. It is, however, possible to use super-resolution approaches to resolve higher densities of RNA molecules (see below).

Super-resolved smFISH

RNA molecules that are too abundant or that concentrate in a small area cannot be resolved by standard microscopy. Structured illumination provides a 2-fold improvement in resolution in each dimension and has been successfully applied to smFISH without experimental modifications (Tantale et al., 2016; Trcek et al., 2015). Interestingly, smFISH can also be combined with expansion microscopy to increase spatial resolution (Chen et al., 2016; Tsanov et al., 2016; Wang et al., 2018; Figure 1B). Here, RNAs are anchored to a swellable polymer, either non-specifically (Chen et al., 2016; Wang et al., 2018) or via the readout sequence (Tsanov et al., 2016). The polymer expands after proteolysis and addition of water, yielding a resolution increase of about 3- to 4-fold in every dimension. While the procedure is more complex, the expanded samples can be directly observed on standard wide-field microscopes, and polymer embedding also reduces background fluorescence.

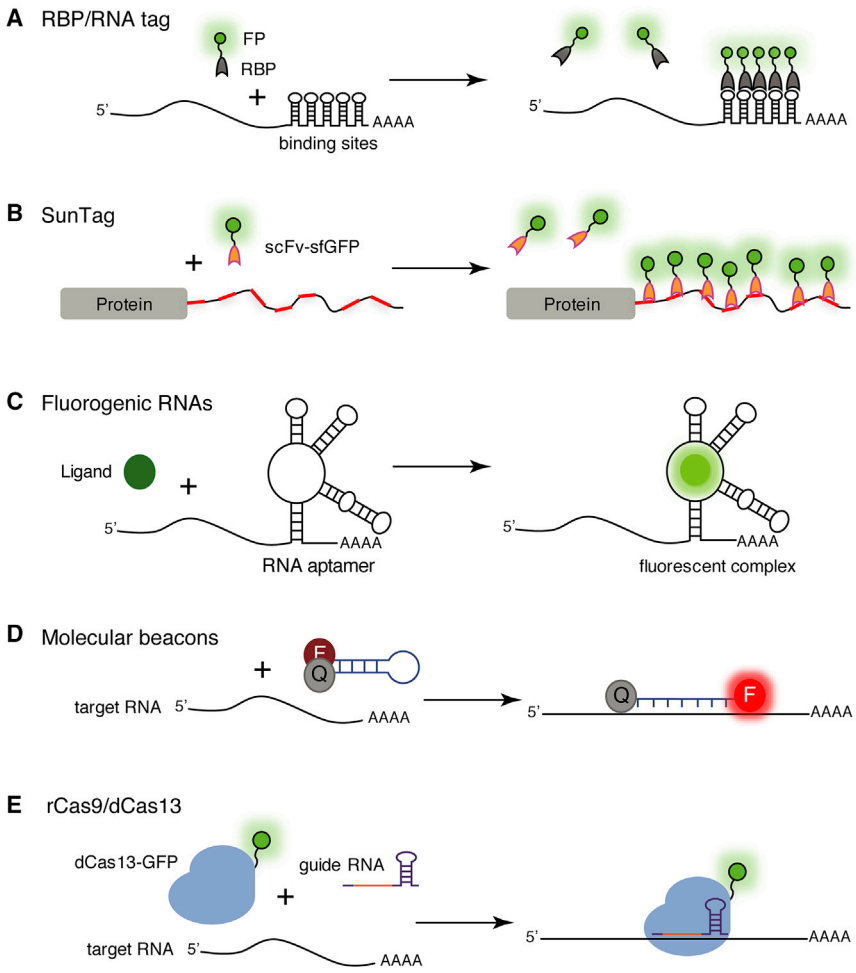

Figure 3. RNA Visualization in Living Cells

(A) RNA-binding protein (RBP) and multimerized tags. An RBP (MCP, PCP, U1A, λN, and BgI; gray) is fused to a fluorescent protein (FP, green) and binds an array of sites engineered into the RNA of interest.

(B) The SunTag system. An array of GCN4 peptide epitopes (red bars) is fused to a protein (gray) while the corresponding scFv-antibody is fused to sfGFP (green).

(C) Fluorogenic RNAs. Dedicated RNA aptamers are inserted in an RNA of interest and promote the fluorescence of small fluorogenic ligands (Hoechst derivatives, DFHBI, TO1-Biotin, and others).

(D) Molecular beacons. Unbound probes fold into a hairpin with a fluorophore (F) in close proximity to a quencher (Q). The quencher moves away upon binding to cellular RNAs.

(E) Programmable RBPs. rCas9 or dCas13 is fused to a fluorescent protein (green) and binds target RNAs in the presence of a guide RNA.

Prospects

Multiplexed smFISH techniques are rapidly evolving and may soon allow a dramatic shift in gene expression studies. In particular, multiplexed smFISH is now an appealing alternative to single-cell sequencing (see Chen et al., 2018b for a comparison of these techniques), with the advantage of having a direct RNA detection method ideally suited for low-abundance RNAs, while providing information on cell shape, micro-environment, and sub-cellular localization. Designing efficient probes is a key step in smFISH. A number of algorithms are available that mostly homogenize the Tm or ΔG° of the probes. However, other factors impact hybridization, including sequence features, base composition, and secondary structure of the probe and target RNAs. These could be included in next-generation design algorithms.

High-throughput and multiplexed datasets provide very rich spatial information, and appropriate image analysis tools are essential to help visualize and interpret these data. First, cells and individual RNA molecules have to be robustly and automatically detected, ideally in 3D. Suitable approaches have been developed for cell lines and multicellular organisms such as *Drosophila* and zebrafish and can be further improved (Mueller et al., 2013; Stapel et al., 2016; Trcek et al., 2015). Second, validated workflows to analyze RNA localization and abundance will be of crucial importance and will ideally include information about the micro-environment of each cell, since it impacts gene expression (Battich et al., 2015).

Imaging Single RNAs in Live Cells

Tag Multimerization

A common strategy to visualize single molecules in live cells uses repeated tags (Figure 3A). These tags bind multiple molecules of a fluorescent detector, thereby revealing single molecules of the target as diffraction-limited spots (see Figures 1C and 1E for examples). Single DNA loci were first visualized using a LacI-GFP fusion and a repetition of 256 *lacO* sites (Robinett et al., 1996). Likewise, RNA molecules were visualized using the coat protein of bacteriophage MS2 (Bertrand et al., 1998; Figure 3A). This protein binds an RNA stem-loop of 19 nucleotides and repetition of 24 such stem-loops in a reporter RNA allows its detection with single-molecule sensitivity (Fusco et al., 2003). More recently, a similar technique (SunTag) was developed for proteins (Tanenbaum et al., 2014; Figure 3B). Here, 12 to 24 repetitions of an epitope are added to the protein of interest and are detected with a monochain antibody fused to GFP.

There are now a number of tag variants that enable multicolor detection of multiple RNA species (reviewed in Tutucci et al., 2018a). In particular, orthogonal RNA labeling can be done with the coat protein of phage PP7 (PCP), as well as the human U1A protein, and the λN and BlgG bacterial anti-terminators. In all these approaches, unbound molecules of detector result in background signal, but this can be reduced by targeting them to a different cellular compartment (Bertrand et al., 1998) or by fine-tuning detector expression (Fusco et al., 2003; Wu et al., 2012). To ensure that the investigated process is not altered by the labeling method, untagged and tagged

RNA can be compared by smFISH, with and without detector expression.

MCP, PCP, and the SunTag have all been optimized for solubility, affinity, and specificity. An advantage of the MCP system is that this RNA-protein interaction has been intensively studied, enabling its fine-tuning for particular applications. Lower affinity variants of the system allow artifact-free studies of RNA metabolism (Tantale et al., 2016; see a detailed study in Tutucci et al., 2018b), while high-affinity mutants provide a long-interaction half-life and are best to study RNA dynamics by FRAP approaches (Boireau et al., 2007; Darzacq et al., 2007). For MCP and PCP, it is also possible to degenerate the binding site sequences to improve RNA folding (Halstead et al., 2015; Tantale et al., 2016; Tutucci et al., 2018b). This also allows the use of more compact repeats and more stem-loops (up to 128), which yield brighter signals. This enables single-molecule detection at low illumination power, thereby minimizing photobleaching and improving long-term RNA imaging (Tantale et al., 2016).

Fluorogenic RNAs

Fluorogenic molecules provide background-free approaches to image RNAs (Figure 3B). The first systems used a Hoechst derivative with an *ad hoc* RNA aptamer (Sando et al., 2007), or the chemical DFHBI and an aptamer called Spinach (Paige et al., 2011). DFHBI does not fluoresce by itself but becomes fluorescent when maintained in a particular conformation, which is achieved upon binding Spinach RNA (Paige et al., 2011). Improvements of the original Spinach include new variants that are shorter and have better folding and photo-physical properties (Filonov et al., 2014). Aptamers for other bright fluorogenic ligands give further diversity and allow multicolor imaging (Autour et al., 2018; Song et al., 2017). Fluorogenic RNAs have not yet been used for single-molecule imaging, but a few experiments showed that they work *in vivo* (Autour et al., 2018; Guet et al., 2015; Song et al., 2017). Single-molecule sensitivity may require improvements in brightness, folding, and cell penetration, and a decrease in non-specific staining.

Visualization of Endogenous, Untagged RNAs

This can be achieved with molecular beacons, whose fluorescence increases upon target binding (Figure 3D). Their design is, however, tedious, and they must be exogenously supplied to the cell. The widely used Cas9 system can be re-purposed to bind and image RNA (Nelles et al., 2016). Recently, analysis of type VI CRISPR-Cas systems revealed that Cas13 enzymes are RNA-programmable RNA-binding proteins (RBPs), and that catalytically inactive Cas13 fused to GFP can be used to image RNA (Cox et al., 2017; Figure 3E). While these tools do not yet allow single-molecule imaging, their simplicity and rapid development offer great promise.

Limitations and Future Developments

There is now a large body of tools to image RNAs in live cells, such that the choice of a particular variant can be tailored to the specific experimental need. An important question is the number of images one can collect while maintaining single-molecule sensitivity. As tentative guidelines for wide-field imaging using MCP-GFP, a hundred MS2 repeats allow for recording thousands of images, while 24 repeats, as in the original design, yield several hundred images (Tantale et al., 2016). Shorter and optimized tags can, however, minimize the risk of biological artifacts (Tutucci et al., 2018b), and the final choice ultimately depends on the user needs and the limitation of the biological system. Large repeats can be powerful when the system is optically challenging as in embryos, or when a high temporal resolution is needed over long time periods, as for transcriptional studies (which moreover often tolerate these tags well). Short and optimized tags are in turn essential if the process of interest becomes disrupted by the insertion of long repeats. It is thus always important to control for the effect of tag introduction.

Future challenges will include developing methods to image single molecules of endogenous untagged RNAs, as well as short RNAs (currently only accessible via microinjection; Pitchiaya et al., 2013). Brighter signals may also foster intra-vital RNA imaging. This may require new labeling/detection methods, new fluorogenic molecules, and signal amplification systems, possibly in combination with bright and photo-stable dyes. Imaging strategies and/or biosensors tailored to specific RNA processing steps may also have significant advantages over all-purpose imaging approaches able to track RNAs from birth to death.

Imaging Heterogeneity in Gene Expression

Transcription Is Bursty

Single-cell measurements provide the ability to observe heterogeneous behaviors that are normally masked by ensemble techniques. Early evidence from Miller chromatin spreads suggested that transcription initiation can occur in an irregular fashion (McKnight and Miller, 1979), and single-molecule approaches in fixed and live cells have now firmly established that transcription initiation is not constant but occurs in so-called bursts (see Nicolas et al., 2017; Patange et al., 2018; Symmons and Raj, 2016 for reviews). Rather qualitatively defined, bursts are periods of transcriptional activity followed by inactive periods, leading to expression heterogeneity even between genetically identical cells. The realization that a central biological process such as transcription can be heterogeneous and stochastic led to important questions (Nicolas et al., 2017; Patange et al., 2018; Symmons and Raj, 2016): how do organisms function despite such variability, and can it provide evolutionary advantages? What are the factors causing and shaping bursts? Can we provide a quantitative understanding of transcription?

Mathematical Modeling Gives Access to the Dynamics of Promoter States

The molecular mechanisms underlying transcriptional bursts have been a central question during the last decade. While no general rules have been identified and the precise behavior likely depends on the gene and organism, some general trends have emerged (Nicolas et al., 2017). Transcription factor dynamics (search time of DNA target sites and their availability; DNA dissociation rates), nuclear architecture (DNA looping, promoter-enhancer contacts, and nuclear compartmentalization), and local chromatin environment (nucleosome occupancy, histone modifications, and number and affinity of regulatory elements) have all been shown to contribute to burst behavior (Nicolas et al., 2017; Patange et al., 2018; Symmons and Raj, 2016). Bursts are often analyzed in terms of amplitude (how strong is transcription during a burst?), frequency (how often do bursts

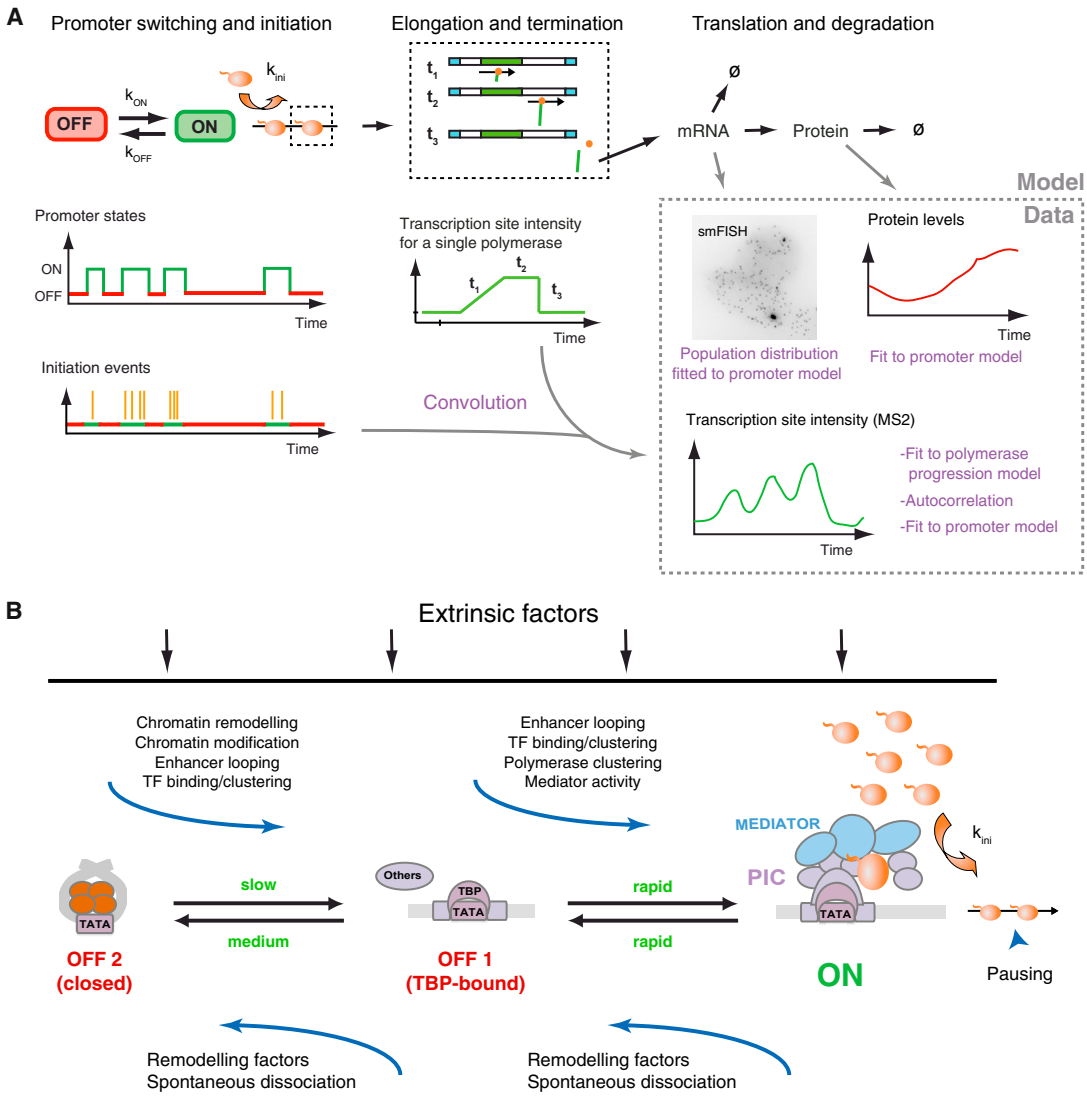

Figure 4. Theoretical and Biochemical Model of Gene Bursting

(A) Model and analyses of gene bursting. Top: model depicting two promoter states (ON and OFF; left), as well as the synthesis and degradation of the corresponding mRNA and encoded protein (middle and right). Left: stochastic, time-dependent switching of promoter state (top and middle) and polymerase firing events (bottom). Central panel: the signal generated by a single polymerase while transcribing an MS2-tagged gene. Right panels: data generated by various approaches and corresponding analyses.

(B) Biochemical model of transcription initiation with putative rates of promoter switches at steady state. Slow, several tens of minutes; medium, several minutes; rapid, tens of seconds. PIC, pre-initiation complex (violet); k_{ini}, initiation rate.

occur?), and duration (how long do bursts last?). These descriptions are useful, but they provide limited mechanistic insights and a more detailed understanding requires mathematical models incorporating active and inactive promoter states (Figure 4A). These states are hidden and fluctuations of promoter activity provide only indirect information. Defining their molecular identity is thus challenging, although crucial to understand transcription initiation (see below). The simplest model is the random telegraph model, whereby a promoter stochastically switches between a transcriptionally silent and an active state (detailed in Munsky et al., 2012; Figure 4A). This model can be parameterized by the promoter switching rates, a transcription and a degradation rate.

Methods and Challenges

Bursting can be studied with different approaches (Figure 4A). smFISH provides absolute counts of mature mRNA, which are often analyzed under the assumption of ergodicity, i.e., that measuring a cell population at a single time point provides the same information as a single cell over many time points. SmFISH can also quantify the amount of nascent RNAs present at the transcription site, and this reflects promoter activity more closely because of the short time nascent RNAs spend there. Using both mature and nascent RNAs captures different timescales of the process and thus provides better constraints for model fitting. Nevertheless, parameter estimation is not always precise, since large parameter ranges can describe the experimental data

(Zenklusen et al., 2008). Live-cell measurements are complementary to smFISH since they provide direct access to the temporal dimension. Fluorescent or luminescent protein reporters are simple to use but lack single-molecule sensitivity and only indirectly report on transcription. Furthermore, RNA and protein half-lives limit the detection of rapid fluctuations (Raj et al., 2006), i.e., occurring in the minute range or shorter. More direct measurements of promoter activity can be achieved by inserting an MS2 or another RNA tag downstream of the promoter of interest (Chubb et al., 2006). By monitoring the intensity of transcription sites over time, promoter activity can be described at timescales ranging from seconds to days. Reaching single-molecule sensitivity is important as it opens the possibility to detect all polymerases entering elongation. If all polymerases behave similarly, transcription site intensities result from the convolution of the signal of a single polymerase by the distribution of initiation events (Figure 4A). The intensity traces can be analyzed by an autocorrelation approach (Larson et al., 2011), or by directly fitting a model describing polymerase progression through the gene (Boireau et al., 2007; Darzacq et al., 2007; Martin et al., 2013). An important challenge is the quantitative comparison of experiments performed with different approaches (protein reporter, smFISH, and RNA reporter) because they differ vastly in temporal resolution, sensitivity, and modeling/data analysis.

While providing insight into transcriptional mechanisms, modeling approaches face several obstacles. An important one is that the common two-state promoter model is an oversimplification of the complex, multi-step process of transcription initiation. Indeed, recent live-cell experiments in Dictyostelium supported a model in which an active promoter state can adopt a continuum of initiation rates (Corrigan et al., 2016), while studies in human cells indicated that promoters fluctuate on multiple timescales, from minutes to hours (Tantale et al., 2016). It seems therefore accurate to devise more complex models including more states or regulatory reactions (Nicolas et al., 2017; see below). However, particular attention should be paid that the model complexity is justified by the available data to avoid overfitting (Patange et al., 2018; Weber et al., 2018). It is also important to use strategies that select the most appropriate model, and ideally a model can be verified by predicting experimentally testable outcomes, or by correlating the impact of experimental perturbations to the different model states (Weber et al., 2018).

Bridging the Gap between Imaging and Biochemistry

Recent genome-wide experiments revealed a variety of complexes forming on core promoters (Krebs et al., 2017; Shao and Zeitlinger, 2017). A key challenge is to understand the relationships between these complexes and the promoter states hypothesized by bursting studies. A related question is how the binding and dissociation rates of promoter-interacting factors relate with the distribution of polymerase initiation events. Depending on the factor, several cases can be envisioned. For factors whose presence is required for initiation (e.g., general transcription factor), their dissociation will switch the promoter into an OFF state. Similarly, binding of repressors or nucleosomes will also set the promoter OFF. Binding kinetics may, however, not always be directly related to initiation. A typical case is when a brief binding provokes a long-lasting effect, as for instance when a stable chromatin modification is introduced by a rapidly dissociating enzyme, or when a factor has many futile binding cycles.

Imaging and biochemical experiments have shown that DNA residence times vary from several tens of minutes for promoter nucleosomes to a few seconds for most transcription factors (reviewed in Deal and Henikoff, 2010; Liu and Tjian, 2018). Interestingly, an intermediate situation is seen with the TATA-binding factor TBP, which provides an anchor to the pre-initiation complex (PIC) and resides on DNA for several minutes (de Graaf et al., 2010; Teves et al., 2018). Notwithstanding other processes, this suggests a minimal kinetic model in which a core promoter could switch stochastically between a few metastable states (Figure 4B): nucleosome-bound, TBP-bound, and initiating. The differential dynamics of these factors suggest that promoter activity may fluctuate on three timescales at steady state (Figure 4B): (1) long inactive periods could depend on the rates of nucleosome association and dissociation from core promoters, which would occur spontaneously or be driven by remodeling enzymes; (2) minute-long periods that are permissive for transcription could be created by TBP binding; and (3) more rapid fluctuations could be determined by steps occurring after TBP binding, and likely related to PIC assembly and polymerase recruitment. Transition between these states may involve several intermediates, branched pathways, and multiple molecular events. These likely include enhancer/promoter contacts, chromatin modification and remodeling, transcription factor binding, and dissociation. Although reductionist, this simplified model nevertheless has some experimental support. First, electron microscopy (EM) images of single molecules of yeast promoters showed a stochastic nucleosome configuration and occupancy even when promoters are active, and it was further shown that nucleosome dynamics impact bursting (Brown et al., 2013). Second, the TATA box of heat-shock genes in yeast determines their degree of noise (Blake et al., 2006), and a recent meta-analysis extended these results by showing that TBP and its binding sequences are major determinants of noise across the yeast genome (Ravarani et al., 2016). Third, in mammalian cells, promoters fluctuate on short and long timescales, and TBP binding was proposed to determine permissive periods of several minutes, while increasing its dissociation rate induces more frequent long OFF periods (Tantale et al., 2016). Finally, RNA polymerase II and Mediator were shown to form transient clusters lasting 5 to more than 150 s (Cisse et al., 2013; Cho et al., 2018). Polymerase clusters precede initiation (Cho et al., 2016), and they may thus be responsible for the most rapid fluctuations of promoter activity, and in particular for the rapid loading of successive polymerases that generate convoys: groups of closely spaced polymerases that transcribe a gene together (Tantale et al., 2016; see also Liu and Tjian, 2018). In further support of this hypothesis, Mediator knockdown has been shown to impair the formation of polymerase convoys, and reducing the size of the polymerase C-terminal repeat both decreases polymerase clustering and prevents efficient initiation in live cells (Boehning et al., 2018; Boireau et al., 2007). Interestingly, these transient clusters likely form by so-called phase-separation mechanisms (Hnisz et al., 2017; Cho et al., 2018; Boehning et al., 2018; Sabari et al., 2018), by which multivalent

low-affinity interactions drive aggregation when the relevant factors reach a critical concentration. The resulting increase in local concentrations may in turn drive series of transcription initiation events.

Another mechanism potentially important for bursting is diffusion by local exploration, which allows a factor to repeatedly visit the same promoter (Izeddin et al., 2014). Interestingly, the pause release factor pTEFb is a local explorer (Izeddin et al., 2014), and promoter-proximal pausing is a major regulatory point in higher eukaryotes. It will thus be interesting to determine how promoter-proximal pausing affects bursting, an important question that is still poorly understood. In the longer run, simultaneous imaging of the factors involved in transcription initiation together with promoter activity will clarify their role in bursting and the mechanisms of transcription initiation. It is, however, worth noting that the slow fluctuations are likely to have major effects on cell phenotypes because rapid fluctuations are generally buffered by mRNA and protein half-lives (Raj et al., 2006). It is also important to note that phenotypic consequences of transcriptional noise can be numerous (Patange et al., 2018; Symmons and Raj, 2016), and include incomplete penetrance of mutations and stochasticity in cell reprogramming, in resistance to therapy in melanomas, in phage and viral latency/reactivation, in cell fate decisions, etc.

Extrinsic Factors Are Another Important Source of Cellular Heterogeneity

Pioneering studies established an important distinction on whether the source of variability is intrinsic or extrinsic to the observed system (Elowitz et al., 2002; Raj et al., 2006). Extrinsic factors, also called "hidden parameters," impact many genes simultaneously (for example, cell cycle, cellular micro-environment, and activation of a pathway). In contrast, intrinsic variability reflects the stochasticity of biochemical reactions involving a small number of molecules, such as switching between promoter states. A key conceptual difference is that extrinsic factors lead to predictable variations, while intrinsic noise is only random. Extrinsic factors leading to cell-to-cell variability must thus be carefully identified, since otherwise the fluctuations can be attributed to intrinsic noise and may confound analyses of promoter dynamics (Patange et al., 2018; Symmons and Raj, 2016). Interestingly, differences in the volume of mammalian cells account for much of the inter-cellular variability in the copy number of mature mRNAs (Battich et al., 2015; Padovan-Merhar et al., 2015). This phenomenon likely allows the maintenance of cellular homeostasis, and its regulation has been proposed to involve transcription and possibly also nuclear export (Battich et al., 2015; Padovan-Merhar et al., 2015). Interestingly, yeast cells use the exonuclease Xrn1 to feed back on transcription and RNA decay when mutations globally affect mRNA concentrations (Haimovich et al., 2013; Sun et al., 2013). It will be interesting to determine whether these mechanisms are evolutionary conserved, and how they control transcription.

Imaging Promoter Activity in Live Embryos

An essential question is the physiological consequences of gene expression noise. Seen from two extreme angles, organisms could either devise strategies to reduce noise or use heterogeneity as an evolutionary advantage to create diversity (Nicolas et al., 2017; Patange et al., 2018; Symmons and Raj, 2016). Studying transcription dynamics in live embryos provides direct access to these questions.

Dynamic Features of Pattern Formation in Drosophila *Embryos*

During development of a multicellular organism, precise control of gene expression allows the reproducible establishment of patterns, which lead to the formation of tissues and organs at the right time and place. By creating synthetic enhancer-MS2-reporter transgenes, several studies in *Drosophila* revealed the precise spatiotemporal regulation of gene expression in developing embryos (Bothma et al., 2014; Garcia et al., 2013; Lucas et al., 2013). For example, visualization of the dynamic activation of the well-characterized eve stripe 2 revealed the ephemeral nature of the stripe (~15 min; Bothma et al., 2014), which was not suspected from decades of fixed-cell studies of the corresponding enhancer.

Imaging promoter activity in living embryos provides precise information about synchrony in gene activation. Some developmental genes are activated in a fast and synchronous manner, in which virtually all nuclei of a given pattern show simultaneous expression, while others exhibit erratic and uncoordinated activation (Boettiger and Levine, 2009). Adopting a synchronous mode of transcriptional activation appears particularly important for morphogenetic processes that require a high coordination between many equivalent cells (Lagha et al., 2013). Interestingly, asynchrony may also be functionally relevant. Quantitative imaging of two major components of the Rho GTPase pathway, which control apical constrictions during mesoderm invagination, revealed the existence of a transcriptional temporal gradient (Lim et al., 2017). Within the presumptive mesoderm where all nuclei are thought to be equivalent, a subset exhibits an early expression of these two components, and these nuclei are the first to undergo coordinated invagination during gastrulation. Bridging the gap between transcriptional dynamics and subsequent cellular events occurring within a tissue is a future challenge of developmental biology.

Transcriptional Memory

Probing gene activation in a developing organism allows tracking the transmission of active transcriptional states from mother to daughter cells through mitosis, herein referred to as "transcriptional memory." Rapid post-mitotic transcriptional re-activation has been documented in a variety of cell lines and is attributed to mitotic bookmarking mechanisms, where some transcription factors remain bound to mitotic DNA (reviewed in Festuccia et al., 2017). However, direct visualization of this memory in a multicellular organism has only been achieved in Dictyostelium (Muramoto et al., 2010) and more recently in early fly embryos (Ferraro et al., 2016). The functional relevance of memory at endogenous loci in *Drosophila* as well as in higher vertebrates is still unknown, although highly suspected. Indeed, mitotic propagation of cell fate decisions in an embryo undergoing rapid cell divisions appears essential to coordinate tissue specifications.

Enhancer-Promoter Communication

To decipher the effects of enhancers on bursting kinetics in *Drosophila*, a two-color MS2/PP7 approach was used to monitor expression of two promoters controlled in *cis* by a shared

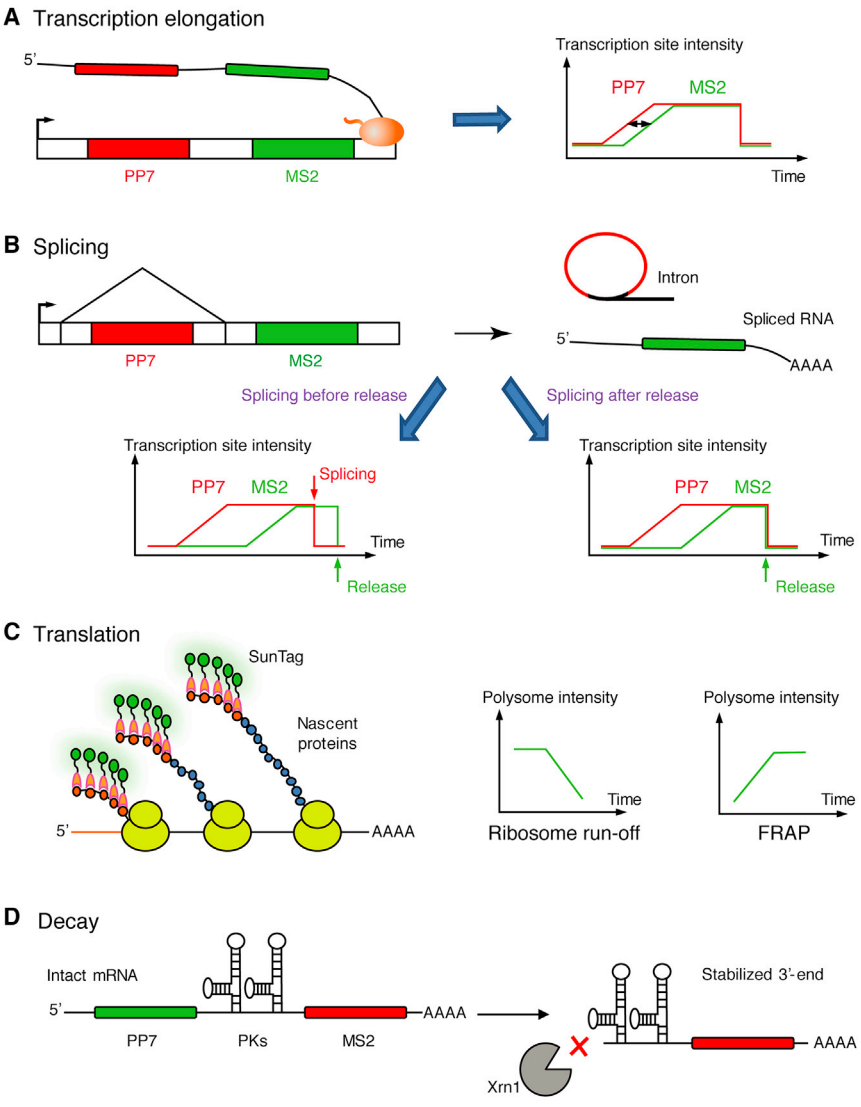

Figure 5. Strategies to Analyze RNA Synthesis and Processing in Living Cells

(A) Transcription elongation. Left: schematic of a two-color reporter with PP7 and MS2 repeats in red and green, respectively, and being transcribed. Right: time traces generated by a single polymerase transcribing the reporter. The arrow points the time delay required for the polymerase to go from the PP7 to the MS2 tag.

(B) Splicing. Top: a two-color splicing reporter generates a PP7-labeled intron and an MS2-labeled spliced RNA. Bottom: time traces generated by a single polymerase transcribing the reporter gene, if splicing is co-transcriptional (left) or post-transcriptional (right).

(C) Translation. Left: schematic of an mRNA reporter for live-cell visualization of translation with the SunTag system. Ribosomes are yellow, the SunTag repeats in orange, and the scFv-sfGFP in light orange and green. Right: intensity of a single polysome after arrest of translation initiation (run-off polysome) or FRAP.

(D) RNA decay. Left: schematic of the TREAT biosensor, with PP7 and MCP repeats in green and red, respectively, and the pseudoknots (PKs) located between the repeats. Right: the 3′ decay intermediate is resistant to Xrn1-mediated exonuclease degradation.

enhancer (Fukaya et al., 2016). Challenging classical models of enhancer-promoter competition, this revealed a surprising coordinate bursting of the two promoters. Physical proximity between enhancer and promoter has recently been shown to precede and to be required for transcriptional activation *in vivo* (Chen et al., 2018a). These data are consistent with current views of transcription as involving transient micro-domains, likely based on enhancer-driven transcription factor clustering and phase separation mechanisms (Hnisz et al., 2017; Liu and Tjian, 2018).

Spatiotemporal Aspects of RNA Metabolism

Gene expression steps are physically and functionally connected, allowing checkpoints, quality controls, coupling, but also competition between parallel reactions. Imaging the relevant kinetics not only gives a timescale for these processes, but also helps in understanding gene regulation at the level of single cells.

Transcription Elongation and 3′ End Formation

The time an RNA spends at its transcription site spans from elongation to 3′ end processing/release. It can be measured by labeling nascent transcripts in live cells and measuring their rate of appearance and disappearance, using either FRAP or natural stochastic variations in promoter activity (Boireau et al., 2007; Darzacq et al., 2007; Larson et al., 2011; Figures 4A and 5A). The relative duration of elongation versus 3′ processing can be further validated by placing probes at different distances from the poly(A) site and measuring their relative intensities or residency times by fixed and live-cell imaging, respectively (Boireau et al., 2007; Larson et al., 2011; Zenklusen et al., 2008; Figure 5A). It is also possible to use bicolor reporters with two tags along the gene. This allows clocking polymerases while they travel from the first to the second tag, and it is a powerful approach to obtain a direct readout of polymerase elongation rates (Fukaya et al., 2017; Hocine et al., 2013; Figure 5A).

In yeast and mammals, 3′ end processing occurs with half-times ranging from 50 to 100 s (Boireau et al., 2007; Larson et al., 2011; Tantale et al., 2016; Zenklusen et al., 2008), although inefficient poly(A) sites are processed much more slowly (Schmidt et al., 2011). Elongation rates are similar in different model organisms and range from 1 to 4.5 kb/min, in agreement with biochemical measurements (Boireau et al., 2007; Corrigan et al., 2016; Darzacq et al., 2007; Garcia et al., 2013; Hocine et al., 2013; Jonkers and Lis, 2015; Larson et al., 2011; Lucas et al., 2013). Interestingly, polymerases, alone or in

convoys, can travel the same gene at different speeds (Hocine et al., 2013; Tantale et al., 2016). The reasons for this are not known but may involve chromatin state, polymerase modifications, DNA topology, or the activity of topoisomerases or histone chaperones.

A wealth of biochemical data indicates that polymerase elongation rates are precisely controlled and play regulatory roles themselves (reviewed in Kwak and Lis, 2013; Naftelberg et al., 2015). Using imaging, it was found that elongation rates vary across the cell cycle (Larson et al., 2011), and that they depend on the phosphorylation status of the polymerase C-terminal domain (Muñoz et al., 2009). Applying these imaging tools to more biological systems will be important to better characterize the relationships between polymerase elongation rates and gene regulation.

Splicing

Splicing rates can be measured by labeling an intron with an MS2 tag and monitoring its dynamics in live cells (Schmidt et al., 2011; Figure 5B). Two-color reporters with intronic and exonic tags detect unspliced and spliced RNA simultaneously, and they also allow determining the fraction of RNA that splices co- and post-transcriptionally (Coulon et al., 2014; Figure 5B). It was found that splicing of the efficient MINX intron is co-transcriptional and takes 2.5–3 min (Schmidt et al., 2011), while the second intron of the β-globin gene takes 4 min (Coulon et al., 2014). Interestingly, this latter intron was found to splice both co- and post-transcriptionally, after release from its transcription site, suggesting a kinetic competition where splicing and 3′ end formation occur as parallel reactions. In agreement, smFISH studies indicate that pre-mRNAs with weak splice sites are processed post-transcriptionally and away from their transcription site (Vargas et al., 2011). It should, however, be noted that in some cases, unspliced mRNAs can also be retained at their transcription sites (Brody et al., 2011). Interestingly, the splicing kinetics of both the MINX and β-globin introns were found to be most consistent with a multi-step model in which splicing times have a narrow distribution, which may be important to coordinate RNA processing reactions (Schmidt et al., 2011).

Another study analyzed the splicing rates of the two β-globin introns as well as different IgM reporters (Martin et al., 2013). By tracking single pre-mRNAs at their transcription site, significantly faster splicing rates were estimated (20–40 s), which correlated with splice site strength. Splicing rates in the minute range are consistent with the dynamics of splicing factors, which reside for tens of seconds at transcription sites (Huranová et al., 2010). This is also consistent with estimates based on EM studies and with the co-transcriptional splicing observed for many introns in transcriptomic studies. Interestingly, nascent RNA sequencing methods revealed that some introns are spliced in very close proximity to their 3′ splice sites in yeast (Oesterreich et al., 2016). Thus, these introns splice rapidly and display a high degree of coupling with transcription. Expanding the repertoire of introns analyzed by live-cell techniques may reveal a range of splicing rates, in connection with splicing regulation and the dynamics of spliceosome assembly. It will be also interesting to determine whether spliceosome assembly can be driven by clustering of splicing factors and phase-separation mechanisms.

Translation

TRICK is a biosensor that identifies mRNAs that have never been translated (Halstead et al., 2015). Recently, four studies showed that the SunTag can be used to directly measure the ribosome load of single mRNPs in living cells (Pichon et al., 2016; Wang et al., 2016; Wu et al., 2016; Yan et al., 2016), and a fifth study achieved a similar result using repeated HA and FLAG tags and fluorescent Fabs (Morisaki et al., 2016). Insertion of these tags at a protein N terminus allows detection of nascent peptides as soon as they emerge from the ribosome, with a sensitivity of single polysomes (Figures 5C and 1E). Single-particle tracking revealed that polysomes diffuse at a rate similar to that of the untranslated mRNAs, and slower when close to the nucleus (Wang et al., 2016). It was discovered that translation of single mRNA fluctuates and shows bursting (Pichon et al., 2016; Wu et al., 2016; Yan et al., 2016). Interestingly, inserting the SunTag into the endogenous *POLR2A* gene revealed smaller fluctuations, suggesting that translation of housekeeping mRNAs may be more robust (Pichon et al., 2016). As for transcription, elongation rates could be estimated by fluctuation analysis or FRAP, and ranged from 3 to 17 aa/s (Pichon et al., 2016; Wu et al., 2016; Yan et al., 2016; Figure 5C). The reason for these variations is not known but may involve codon usage, RNA secondary structures, obstacles such as RBPs, and technical differences. Two localized mRNAs were also analyzed: β-actin mRNA, which is transported to dendrites in neurons (Wu et al., 2016), and the large dynein subunit mRNA, which accumulates in cytoplasmic RNA aggregates (Pichon et al., 2016). Surprisingly, it was found that both mRNAs were translated while being transported by motors, indicating that transport and translation are not mutually exclusive as previously thought. In addition, the dynein mRNA aggregates were shown to be specialized translation factories (Pichon et al., 2016), suggesting that translation may be highly compartmentalized in human cells. Such factories may also allow mRNAs to be translated by specialized machineries, including specialized ribosomes.

RNA Decay

TREAT is a biosensor that was recently engineered to study RNA decay (Horvathova et al., 2017; Figure 5D). By introducing a viral pseudoknot element between PP7 and MS2 stem-loops, it was possible to stabilize and visualize degradation intermediates containing the 3′ part of the RNA (Horvathova et al., 2017). Two-color, single RNA imaging allows distinguishing full-length RNAs (PCP and MCP positive) from 3′ degradation products (PCP negative and MCP positive). Using this system, degradation was found to be a single-step Poisson process, and it was also possible to image Ago2-dependent slicing in real time by monitoring the dissociation of PCP and MCP signals. Using this tool, it thus becomes possible to determine where and when RNAs are degraded in living cells.

Prospects

A number of live-cell, single-molecule tools are now available to image RNA metabolism from synthesis to decay. These approaches revealed the dynamic and stochastic nature of gene expression processes, and simultaneous imaging of RNA molecules and the relevant *trans*-acting factors should bring a new level of understanding of the mechanisms at play. It will also

be important to increase both the throughput and robustness of these approaches, in order to study more genes and to access the vast number of regulatory mechanisms operating in living cells. RNA imaging has been successful in live *Drosophila* embryos, but single-molecule experiments remain very challenging in this organism. Increasing the sensitivity of RNA imaging techniques may thus open new doors to analyze gene expression in tissues and multicellular organisms, by allowing single-molecule sensitivity in these demanding biological systems.

ACKNOWLEDGMENTS

We thank Evelina Tutucci and Adrien Senecal for critical readings of the manuscript. X.P. was support by a fellowship from the LABEX Epigenemed. This work was supported by grants from the ANR (ANR-14-CE10-0018-01), the FRM, and the ANRS, and by the ERC starting grant to M.L. (SYNC_DEV_679792).

DECLARATION OF INTERESTS

The authors declare no competing interests.

REFERENCES

Autour, A., C Y Jeng, S., D Cawte, A., Abdolahzadeh, A., Galli, A., Panchapakesan, S.S.S., Rueda, D., Ryckelynck, M., and Unrau, P.J. (2018). Fluorogenic RNA Mango aptamers for imaging small non-coding RNAs in mammalian cells. Nat. Commun. *9*, 656.

Battich, N., Stoeger, T., and Pelkmans, L. (2013). Image-based transcriptomics in thousands of single human cells at single-molecule resolution. Nat. Methods *10*, 1127–1133.

Battich, N., Stoeger, T., and Pelkmans, L. (2015). Control of transcript variability in single mammalian cells. Cell *163*, 1596–1610.

Bertrand, E., Chartrand, P., Schaefer, M., Shenoy, S.M., Singer, R.H., and Long, R.M. (1998). Localization of ASH1 mRNA particles in living yeast. Mol. Cell *2*, 437–445.

Blake, W.J., Balázsi, G., Kohanski, M.A., Isaacs, F.J., Murphy, K.F., Kuang, Y., Cantor, C.R., Walt, D.R., and Collins, J.J. (2006). Phenotypic consequences of promoter-mediated transcriptional noise. Mol. Cell *24*, 853–865.

Boehning, M., Dugast-Darzacq, X., Rankovic, M., Hansen, A.S., Tae-Kyung, Y., Marie-Nelly, H., Kokic, G., Dailey, G.M., Cramer, P., Darzacq, X., and Zweckstetter, M. (2018). RNA polymerase II clustering through CTD phase separation. bioRxiv. https://doi.org/10.1101/316372.

Boettiger, A.N., and Levine, M. (2009). Synchronous and stochastic patterns of gene activation in the Drosophila embryo. Science *325*, 471–473.

Boireau, S., Maiuri, P., Basyuk, E., de la Mata, M., Knezevich, A., Pradet-Balade, B., Bäcker, V., Kornblihtt, A., Marcello, A., and Bertrand, E. (2007). The transcriptional cycle of HIV-1 in real-time and live cells. J. Cell Biol. *179*, 291–304.

Bothma, J.P., Garcia, H.G., Esposito, E., Schlissel, G., Gregor, T., and Levine, M. (2014). Dynamic regulation of eve stripe 2 expression reveals transcriptional bursts in living Drosophila embryos. Proc. Natl. Acad. Sci. USA *111*, 10598–10603.

Brody, Y., Neufeld, N., Bieberstein, N., Causse, S.Z., Böhnlein, E.M., Neugebauer, K.M., Darzacq, X., and Shav-Tal, Y. (2011). The in vivo kinetics of RNA polymerase II elongation during co-transcriptional splicing. PLoS Biol. *9*, e1000573.

Brown, C.R., Mao, C., Falkovskaia, E., Jurica, M.S., and Boeger, H. (2013). Linking stochastic fluctuations in chromatin structure and gene expression. PLoS Biol. *11*, e1001621.

Chen, K.H., Boettiger, A.N., Moffitt, J.R., Wang, S., and Zhuang, X. (2015). RNA imaging. Spatially resolved, highly multiplexed RNA profiling in single cells. Science *348*, aaa6090.

Chen, F., Wassie, A.T., Cote, A.J., Sinha, A., Alon, S., Asano, S., Daugharthy, E.R., Chang, J.B., Marblestone, A., Church, G.M., et al. (2016). Nanoscale imaging of RNA with expansion microscopy. Nat. Methods *13*, 679–684.

Chen, H., Levo, M., Barinov, L., Fujioka, M., Jaynes, J.B., and Gregor, T. (2018a). Dynamic interplay between enhancer-promoter topology and gene activity. Nat. Genet. Published online July 23, 2018. https://doi.org/10.1038/s41588-018-0175-z.

Chen, X., Teichmann, S., and Meyer, K. (2018b). From tissues to cell types and back: single-cell gene expression analysis of tissues architecture. Annu. Rev. Biomed. Data Sci. *1*, 29–51.

Cho, W.K., Jayanth, N., English, B.P., Inoue, T., Andrews, J.O., Conway, W., Grimm, J.B., Spille, J.H., Lavis, L.D., Lionnet, T., and Cisse, I.I. (2016). RNA polymerase II cluster dynamics predict mRNA output in living cells. eLife *5*, e13617.

Cho, W.K., Spille, J.H., Hecht, M., Lee, C., Li, C., Grube, V., and Cisse, I.I. (2018). Mediator and RNA polymerase II clusters associate in transcription-dependent condensates. Science, eaar4199.

Choi, H.M., Chang, J.Y., Trinh, A., Padilla, J.E., Fraser, S.E., and Pierce, N.A. (2010). Programmable in situ amplification for multiplexed imaging of mRNA expression. Nat. Biotechnol. *28*, 1208–1212.

Chubb, J.R., Trcek, T., Shenoy, S.M., and Singer, R.H. (2006). Transcriptional pulsing of a developmental gene. Curr. Biol. *16*, 1018–1025.

Cisse, I.I., Izeddin, I., Causse, S.Z., Boudarene, L., Senecal, A., Muresan, L., Dugast-Darzacq, C., Hajj, B., Dahan, M., and Darzacq, X. (2013). Real-time dynamics of RNA polymerase II clustering in live human cells. Science *341*, 664–667.

Corrigan, A.M., Tunnacliffe, E., Cannon, D., and Chubb, J.R. (2016). A continuum model of transcriptional bursting. eLife *5*, e13051.

Coulon, A., Ferguson, M.L., de Turris, V., Palangat, M., Chow, C.C., and Larson, D.R. (2014). Kinetic competition during the transcription cycle results in stochastic RNA processing. eLife *3*, e03993.

Cox, D.B.T., Gootenberg, J.S., Abudayyeh, O.O., Franklin, B., Kellner, M.J., Joung, J., and Zhang, F. (2017). RNA editing with CRISPR-Cas13. Science *358*, 1019–1027.

Darzacq, X., Shav-Tal, Y., de Turris, V., Brody, Y., Shenoy, S.M., Phair, R.D., and Singer, R.H. (2007). In vivo dynamics of RNA polymerase II transcription. Nat. Struct. Mol. Biol. *14*, 796–806.

de Graaf, P., Mousson, F., Geverts, B., Scheer, E., Tora, L., Houtsmuller, A.B., and Timmers, H.T. (2010). Chromatin interaction of TATA-binding protein is dynamically regulated in human cells. J. Cell Sci. *123*, 2663–2671.

Deal, R.B., and Henikoff, S. (2010). Capturing the dynamic epigenome. Genome Biol. *11*, 218.

Elowitz, M.B., Levine, A.J., Siggia, E.D., and Swain, P.S. (2002). Stochastic gene expression in a single cell. Science *297*, 1183–1186.

Femino, A.M., Fay, F.S., Fogarty, K., and Singer, R.H. (1998). Visualization of single RNA transcripts in situ. Science *280*, 585–590.

Ferraro, T., Esposito, E., Mancini, L., Ng, S., Lucas, T., Coppey, M., Dostatni, N., Walczak, A.M., Levine, M., and Lagha, M. (2016). Transcriptional memory in the Drosophila embryo. Curr. Biol. *26*, 212–218.

Festuccia, N., Gonzalez, I., Owens, N., and Navarro, P. (2017). Mitotic bookmarking in development and stem cells. Development *144*, 3633–3645.

Filonov, G.S., Moon, J.D., Svensen, N., and Jaffrey, S.R. (2014). Broccoli: rapid selection of an RNA mimic of green fluorescent protein by fluorescence-based selection and directed evolution. J. Am. Chem. Soc. *136*, 16299–16308.

Fukaya, T., Lim, B., and Levine, M. (2016). Enhancer control of transcriptional bursting. Cell *166*, 358–368.

Fukaya, T., Lim, B., and Levine, M. (2017). Rapid rates of Pol II elongation in the Drosophila embryo. Curr. Biol. *27*, 1387–1391.

Fusco, D., Accornero, N., Lavoie, B., Shenoy, S.M., Blanchard, J.M., Singer, R.H., and Bertrand, E. (2003). Single mRNA molecules demonstrate probabilistic movement in living mammalian cells. Curr. Biol. *13*, 161–167.

Gall, J.G., and Pardue, M.L. (1969). Formation and detection of RNA-DNA hybrid molecules in cytological preparations. Proc. Natl. Acad. Sci. USA *63*, 378–383.

Garcia, H.G., Tikhonov, M., Lin, A., and Gregor, T. (2013). Quantitative imaging of transcription in living Drosophila embryos links polymerase activity to patterning. Curr. Biol. *23*, 2140–2145.

Guet, D., Burns, L.T., Maji, S., Boulanger, J., Hersen, P., Wente, S.R., Salamero, J., and Dargemont, C. (2015). Combining Spinach-tagged RNA and gene localization to image gene expression in live yeast. Nat. Commun. *6*, 8882.

Haimovich, G., Medina, D.A., Causse, S.Z., Garber, M., Millán-Zambrano, G., Barkai, O., Chávez, S., Pérez-Ortín, J.E., Darzacq, X., and Choder, M. (2013). Gene expression is circular: factors for mRNA degradation also foster mRNA synthesis. Cell *153*, 1000–1011.

Halstead, J.M., Lionnet, T., Wilbertz, J.H., Wippich, F., Ephrussi, A., Singer, R.H., and Chao, J.A. (2015). Translation. An RNA biosensor for imaging the first round of translation from single cells to living animals. Science *347*, 1367–1671.

Hnisz, D., Shrinivas, K., Young, R.A., Chakraborty, A.K., and Sharp, P.A. (2017). A phase separation model for transcriptional control. Cell *169*, 13–23.

Hocine, S., Raymond, P., Zenklusen, D., Chao, J.A., and Singer, R.H. (2013). Single-molecule analysis of gene expression using two-color RNA labeling in live yeast. Nat. Methods *10*, 119–121.

Horvathova, I., Voigt, F., Kotrys, A.V., Zhan, Y., Artus-Revel, C.G., Eglinger, J., Stadler, M.B., Giorgetti, L., and Chao, J.A. (2017). The dynamics of mRNA turnover revealed by single-molecule imaging in single cells. Mol. Cell *68*, 615–625.e9.

Huranová, M., Ivani, I., Benda, A., Poser, I., Brody, Y., Hof, M., Shav-Tal, Y., Neugebauer, K.M., and Stanek, D. (2010). The differential interaction of snRNPs with pre-mRNA reveals splicing kinetics in living cells. J. Cell Biol. *191*, 75–86.

Izeddin, I., Récamier, V., Bosanac, L., Cissé, I.I., Boudarene, L., Dugast-Darzacq, C., Proux, F., Bénichou, O., Voituriez, R., Bensaude, O., et al. (2014). Single-molecule tracking in live cells reveals distinct target-search strategies of transcription factors in the nucleus. eLife *3*, e02230.

Jonkers, I., and Lis, J.T. (2015). Getting up to speed with transcription elongation by RNA polymerase II. Nat. Rev. Mol. Cell Biol. *16*, 167–177.

Krebs, A.R., Imanci, D., Hoerner, L., Gaidatzis, D., Burger, L., and Schübeler, D. (2017). Genome-wide single-molecule footprinting reveals high RNA polymerase II turnover at paused promoters. Mol. Cell *67*, 411–422.e4.

Kwak, H., and Lis, J.T. (2013). Control of transcriptional elongation. Annu. Rev. Genet. *47*, 483–508.

Lagha, M., Bothma, J.P., Esposito, E., Ng, S., Stefanik, L., Tsui, C., Johnston, J., Chen, K., Gilmour, D.S., Zeitlinger, J., and Levine, M.S. (2013). Paused Pol II coordinates tissue morphogenesis in the Drosophila embryo. Cell *153*, 976–987.

Larson, D.R., Zenklusen, D., Wu, B., Chao, J.A., and Singer, R.H. (2011). Real-time observation of transcription initiation and elongation on an endogenous yeast gene. Science *332*, 475–478.

Larsson, C., Grundberg, I., Söderberg, O., and Nilsson, M. (2010). In situ detection and genotyping of individual mRNA molecules. Nat. Methods *7*, 395–397.

Lécuyer, E., Yoshida, H., Parthasarathy, N., Alm, C., Babak, T., Cerovina, T., Hughes, T.R., Tomancak, P., and Krause, H.M. (2007). Global analysis of mRNA localization reveals a prominent role in organizing cellular architecture and function. Cell *131*, 174–187.

Lim, B., Levine, M., and Yamazaki, Y. (2017). Transcriptional pre-patterning of Drosophila gastrulation. Curr. Biol. *27*, 286–290.

Liu, Z., and Tjian, R. (2018). Visualizing transcription factor dynamics in living cells. J. Cell Biol. *217*, 1181–1191.

Long, X., Colonell, J., Wong, A.M., Singer, R.H., and Lionnet, T. (2017). Quantitative mRNA imaging throughout the entire Drosophila brain. Nat. Methods *14*, 703–706.

Lubeck, E., Coskun, A.F., Zhiyentayev, T., Ahmad, M., and Cai, L. (2014). Single-cell in situ RNA profiling by sequential hybridization. Nat. Methods *11*, 360–361.

Lucas, T., Ferraro, T., Roelens, B., De Las Heras Chanes, J., Walczak, A.M., Coppey, M., and Dostatni, N. (2013). Live imaging of bicoid-dependent transcription in Drosophila embryos. Curr. Biol. *23*, 2135–2139.

Martin, R.M., Rino, J., Carvalho, C., Kirchhausen, T., and Carmo-Fonseca, M. (2013). Live-cell visualization of pre-mRNA splicing with single-molecule sensitivity. Cell Rep. *4*, 1144–1155.

McKnight, S.L., and Miller, O.L., Jr. (1979). Post-replicative nonribosomal transcription units in D. melanogaster embryos. Cell *17*, 551–563.

Mili, S., Moissoglu, K., and Macara, I.G. (2008). Genome-wide screen reveals APC-associated RNAs enriched in cell protrusions. Nature *453*, 115–119.

Moffitt, J.R., Hao, J., Bambah-Mukku, D., Lu, T., Dulac, C., and Zhuang, X. (2016). High-performance multiplexed fluorescence in situ hybridization in culture and tissue with matrix imprinting and clearing. Proc. Natl. Acad. Sci. USA *113*, 14456–14461.

Morisaki, T., Lyon, K., DeLuca, K.F., DeLuca, J.G., English, B.P., Zhang, Z., Lavis, L.D., Grimm, J.B., Viswanathan, S., Looger, L.L., et al. (2016). Real-time quantification of single RNA translation dynamics in living cells. Science *352*, 1425–1429.

Mueller, F., Senecal, A., Tantale, K., Marie-Nelly, H., Ly, N., Collin, O., Basyuk, E., Bertrand, E., Darzacq, X., and Zimmer, C. (2013). FISH-quant: automatic counting of transcripts in 3D FISH images. Nat. Methods *10*, 277–278.

Muñoz, M.J., Pérez Santangelo, M.S., Paronetto, M.P., de la Mata, M., Pelisch, F., Boireau, S., Glover-Cutter, K., Ben-Dov, C., Blaustein, M., Lozano, J.J., et al. (2009). DNA damage regulates alternative splicing through inhibition of RNA polymerase II elongation. Cell *137*, 708–720.

Munsky, B., Neuert, G., and van Oudenaarden, A. (2012). Using gene expression noise to understand gene regulation. Science *336*, 183–187.

Muramoto, T., Müller, I., Thomas, G., Melvin, A., and Chubb, J.R. (2010). Methylation of H3K4 Is required for inheritance of active transcriptional states. Curr. Biol. *20*, 397–406.

Naftelberg, S., Schor, I.E., Ast, G., and Kornblihtt, A.R. (2015). Regulation of alternative splicing through coupling with transcription and chromatin structure. Annu. Rev. Biochem. *84*, 165–198.

Nelles, D.A., Fang, M.Y., O'Connell, M.R., Xu, J.L., Markmiller, S.J., Doudna, J.A., and Yeo, G.W. (2016). Programmable RNA tracking in live cells with CRISPR/Cas9. Cell *165*, 488–496.

Nicolas, D., Phillips, N.E., and Naef, F. (2017). What shapes eukaryotic transcriptional bursting? Mol. Biosyst. *13*, 1280–1290.

Oesterreich, F.C., Herzel, L., Straube, K., Hujer, K., Howard, J., and Neugebauer, K.M. (2016). Splicing of nascent RNA coincides with intron exit from RNA polymerase II. Cell *165*, 372–381.

Padovan-Merhar, O., Nair, G.P., Biaesch, A.G., Mayer, A., Scarfone, S., Foley, S.W., Wu, A.R., Churchman, L.S., Singh, A., and Raj, A. (2015). Single mammalian cells compensate for differences in cellular volume and DNA copy number through independent global transcriptional mechanisms. Mol. Cell *58*, 339–352.

Paige, J.S., Wu, K.Y., and Jaffrey, S.R. (2011). RNA mimics of green fluorescent protein. Science *333*, 642–646.

Patange, S., Girvan, M., and Larson, D.R. (2018). Single-cell systems biology: probing the basic unit of information flow. Curr Opin Syst Biol *8*, 7–15.

Pichon, X., Bastide, A., Safieddine, A., Chouaib, R., Samacoits, A., Basyuk, E., Peter, M., Mueller, F., and Bertrand, E. (2016). Visualization of single endogenous polysomes reveals the dynamics of translation in live human cells. J. Cell Biol. *214*, 769–781.

Pitchiaya, S., Krishnan, V., Custer, T.C., and Walter, N.G. (2013). Dissecting non-coding RNA mechanisms in cellulo by single-molecule high-resolution localization and counting. Methods *63*, 188–199.

Raj, A., Peskin, C.S., Tranchina, D., Vargas, D.Y., and Tyagi, S. (2006). Stochastic mRNA synthesis in mammalian cells. PLoS Biol. *4*, e309.

Raj, A., van den Bogaard, P., Rifkin, S.A., van Oudenaarden, A., and Tyagi, S. (2008). Imaging individual mRNA molecules using multiple singly labeled probes. Nat. Methods *5*, 877–879.

Ravarani, C.N., Chalancon, G., Breker, M., de Groot, N.S., and Babu, M.M. (2016). Affinity and competition for TBP are molecular determinants of gene expression noise. Nat. Commun. *7*, 10417.

Robinett, C.C., Straight, A., Li, G., Willhelm, C., Sudlow, G., Murray, A., and Belmont, A.S. (1996). In vivo localization of DNA sequences and visualization of large-scale chromatin organization using lac operator/repressor recognition. J. Cell Biol. *135*, 1685–1700.

Rouhanifard, S.H., Dunagin, M., Mellis, I.A., Bayatpour, S., Symmons, O., Cote, A., and Raj, A. (2017). Single-molecule fluorescent amplification of RNA using clampFISH probes. bioRxiv. https://doi.org/10.1101/222794.

Sabari, B.R., Dall'Agnese, A., Boija, A., Klein, I.A., Coffey, E.L., Shrinivas, K., Abraham, B.J., Hannett, N.M., Zamudio, A.V., Manteiga, J.C., et al. (2018). Coactivator condensation at super-enhancers links phase separation and gene control. Science, eaar3958.

Sando, S., Narita, A., and Aoyama, Y. (2007). Light-up Hoechst-DNA aptamer pair: generation of an aptamer-selective fluorophore from a conventional DNA-staining dye. ChemBioChem *8*, 1795–1803.

Schmidt, U., Basyuk, E., Robert, M.C., Yoshida, M., Villemin, J.P., Auboeuf, D., Aitken, S., and Bertrand, E. (2011). Real-time imaging of cotranscriptional splicing reveals a kinetic model that reduces noise: implications for alternative splicing regulation. J. Cell Biol. *193*, 819–829.

Shah, S., Lubeck, E., Schwarzkopf, M., He, T.F., Greenbaum, A., Sohn, C.H., Lignell, A., Choi, H.M., Gradinaru, V., Pierce, N.A., and Cai, L. (2016). Single-molecule RNA detection at depth by hybridization chain reaction and tissue hydrogel embedding and clearing. Development *143*, 2862–2867.

Shah, S., Takei, Y., Zhou, W., Lubeck, E., Yun, J., Eng, C.L., Koulena, N., Cronin, C., Karp, C., Liaw, E.J., et al. (2018). Dynamics and Spatial Genomics of the Nascent Transcriptome by Intron seqFISH. Cell *174*, 363–376.e16.

Shao, W., and Zeitlinger, J. (2017). Paused RNA polymerase II inhibits new transcriptional initiation. Nat. Genet. *49*, 1045–1051.

Sinnamon, J.R., and Czaplinski, K. (2014). RNA detection in situ with FISH-STICs. RNA *20*, 260–266.

Song, W., Filonov, G.S., Kim, H., Hirsch, M., Li, X., Moon, J.D., and Jaffrey, S.R. (2017). Imaging RNA polymerase III transcription using a photostable RNA-fluorophore complex. Nat. Chem. Biol. *13*, 1187–1194.

Stapel, L.C., Lombardot, B., Broaddus, C., Kainmueller, D., Jug, F., Myers, E.W., and Vastenhouw, N.L. (2016). Automated detection and quantification of single RNAs at cellular resolution in zebrafish embryos. Development *143*, 540–546.

Sun, M., Schwalb, B., Pirkl, N., Maier, K.C., Schenk, A., Failmezger, H., Tresch, A., and Cramer, P. (2013). Global analysis of eukaryotic mRNA degradation reveals Xrn1-dependent buffering of transcript levels. Mol. Cell *52*, 52–62.

Sylwestrak, E.L., Rajasethupathy, P., Wright, M.A., Jaffe, A., and Deisseroth, K. (2016). Multiplexed intact-tissue transcriptional analysis at cellular resolution. Cell *164*, 792–804.

Symmons, O., and Raj, A. (2016). What's luck got to do with it: single cells, multiple fates, and biological nondeterminism. Mol. Cell *62*, 788–802.

Tanenbaum, M.E., Gilbert, L.A., Qi, L.S., Weissman, J.S., and Vale, R.D. (2014). A protein-tagging system for signal amplification in gene expression and fluorescence imaging. Cell *159*, 635–646.

Tantale, K., Mueller, F., Kozulic-Pirher, A., Lesne, A., Victor, J.M., Robert, M.C., Capozi, S., Chouaib, R., Bäcker, V., Mateos-Langerak, J., et al. (2016). A single-molecule view of transcription reveals convoys of RNA polymerases and multi-scale bursting. Nat. Commun. *7*, 12248.

Teves, S.S., An, L., Bhargava-Shah, A., Xie, L., Darzacq, X., and Tjian, R. (2018). A stable mode of bookmarking by TBP recruits RNA polymerase II to mitotic chromosomes. eLife *7*, e35621.

Trcek, T., Grosch, M., York, A., Shroff, H., Lionnet, T., and Lehmann, R. (2015). Drosophila germ granules are structured and contain homotypic mRNA clusters. Nat. Commun. *6*, 7962.

Tsanov, N., Samacoits, A., Chouaib, R., Traboulsi, A.M., Gostan, T., Weber, C., Zimmer, C., Zibara, K., Walter, T., Peter, M., et al. (2016). smiFISH and FISH-quant - a flexible single RNA detection approach with super-resolution capability. Nucleic Acids Res. *44*, e165.

Tutucci, E., Livingston, N.M., Singer, R.H., and Wu, B. (2018a). Imaging mRNA in vivo, from birth to death. Annu. Rev. Biophys. *47*, 85–106.

Tutucci, E., Vera, M., Biswas, J., Garcia, J., Parker, R., and Singer, R.H. (2018b). An improved MS2 system for accurate reporting of the mRNA life cycle. Nat. Methods *15*, 81–89.

Vargas, D.Y., Shah, K., Batish, M., Levandoski, M., Sinha, S., Marras, S.A., Schedl, P., and Tyagi, S. (2011). Single-molecule imaging of transcriptionally coupled and uncoupled splicing. Cell *147*, 1054–1065.

Wang, F., Flanagan, J., Su, N., Wang, L.C., Bui, S., Nielson, A., Wu, X., Vo, H.T., Ma, X.J., and Luo, Y. (2012). RNAscope: a novel in situ RNA analysis platform for formalin-fixed, paraffin-embedded tissues. J. Mol. Diagn. *14*, 22–29.

Wang, C., Han, B., Zhou, R., and Zhuang, X. (2016). Real-time imaging of translation on single mRNA transcripts in live cells. Cell *165*, 990–1001.

Wang, G., Moffitt, J.R., and Zhuang, X. (2018). Multiplexed imaging of high-density libraries of RNAs with MERFISH and expansion microscopy. Sci. Rep. *8*, 4847.

Weber, L., Raymond, W., and Munsky, B. (2018). Identification of gene regulation models from single-cell data. Phys. Biol. *15*, 055001.

Wu, B., Chao, J.A., and Singer, R.H. (2012). Fluorescence fluctuation spectroscopy enables quantitative imaging of single mRNAs in living cells. Biophys. J. *102*, 2936–2944.

Wu, B., Eliscovich, C., Yoon, Y.J., and Singer, R.H. (2016). Translation dynamics of single mRNAs in live cells and neurons. Science *352*, 1430–1435.

Yan, X., Hoek, T.A., Vale, R.D., and Tanenbaum, M.E. (2016). Dynamics of translation of single mRNA molecules in vivo. Cell *165*, 976–989.

Zenklusen, D., Larson, D.R., and Singer, R.H. (2008). Single-RNA counting reveals alternative modes of gene expression in yeast. Nat. Struct. Mol. Biol. *15*, 1263–1271.